Journal of Aquatic and Terrestrial **Ecosystems**

3(3)

Received: July 20, 2025 Accepted: September 09, 2025 Published: September 23, 2025



Effects of Adsorbent Dosage and Particle Size on Fluoride Removal Using Calcium-Spiked Moringa oleifera Seed Powder

Chavaregi Geoffrey, Lusweti Kituyi John and Kipkemboi Keronei Pius

Department of Chemistry & Biochemistry, School of Science, University of Eldoret. PO Box 1125-30100, Eldoret, Kenya

Abstract

Access to safe drinking water remains a major challenge in fluoride-endemic regions, where excessive fluoride concentrations can lead to dental and skeletal fluorosis. This study evaluated the effects of adsorbent dosage, particle size, and particle size classification (mesh size) on the fluoride removal performance of Moringa oleifera seed powder (MOSP) in both calcium-spiked and non-spiked forms. A three-factor factorial batch adsorption experiment was conducted using initial fluoride concentration of 1ppm, dosages of 0.25-2.0 g/100 mL, particle sizes of <250 µm, $250-500 \, \mu m$, and $>500 \, \mu m$, and mesh classifications of 20 (850 μm), 40 (425 μm), and 60(250 µm). Response variables included fluoride removal efficiency, residual fluoride concentration, and adsorption capacity (ge), measured using a fluoride ion-selective electrode. ANOVA and linear regression were applied to evaluate the dose and size response relationships. Results showed that calcium-spiked MOSP consistently outperformed non-spiked MOSP across all parameters. Fluoride removal efficiency increased with dosage, reaching 88.95% for spiked and 70.34% for non-spiked MOSP at 2.0 g. Finer particle sizes and smaller mesh fractions significantly enhanced removal efficiency and reduced residual fluoride levels, with spiked MOSP at ≤250 µm achieving 89.80% removal and residual fluoride below WHO guidelines. Regression analysis confirmed strong inverse relationships between particle size/mesh size and fluoride removal performance, and positive correlations with dosage. The improved performance of calcium-spiked MOSP is attributed to increased surface-active Ca²⁺ sites enabling precipitation of CaF₂ and enhanced adsorption via electrostatic attraction and ion exchange. These findings indicate that calcium-spiked MOSP, optimally prepared at fine particle size and moderate dosage, is a viable, locally sourced defluoridation medium suitable for rural water treatment systems.

Keywords: Fluoride removal, *moringa oleifera*, calcium spiking, biosorption, adsorption efficiency, defluoridation, drinking water safety, Kenya

Journal ISSN: 2960-1118

Issue DOI: https://doi.org/10.69897/jatems.v3i3

Correspondence: <u>jfcom@proton.me</u>

Copyright © 2025 Chavaregi et al. This is an open-access article distributed under the terms of the Creative Commons Attribution License (CC BY).

Funding: The author received no financial support for the research, authorship and/or publication of this article.

Data Availability Statement: The authors confirm that the data supporting the findings of this study are available within the article [and/or] its supplementary materials or upon reasonable request.

Competing interests: The authors declare no potential conflicts of interest with respect to the research, authorship and/or publication of this article.

Introduction

Access to potable water of acceptable chemical quality remains a pressing challenge in many developing regions, where naturally occurring groundwater contaminants such as fluoride persist due to geochemical processes (Rasool et al., 2018). In Sub-Saharan Africa and South Asia, prolonged water–rock interactions release fluoride-bearing minerals into aguifers, a process driven by dissolution kinetics and mineral-water equilibrium reactions (Onipe et al., 2020). Although fluoride is beneficial in trace amounts for dental health, concentrations exceeding the World Health Organization (WHO) guideline of 1.5 mg/L cause chemical toxicity that manifests as dental and skeletal fluorosis (Kabir et al., 2020; Ghosh et al., 2013). Chronic overexposure disrupts normal mineralization pathways in bones and teeth, leading to structural changes in hydroxyapatite lattices, joint stiffness, and bone deformities (Fina & Rigalli, 2015; Choubisa, 2024).

Kenya is among the most affected countries, with groundwater in parts of the Rift Valley and Western Kenya frequently exceeding 10 mg/L fluoride (Rusiniak et al., 2021). The high fluoride concentrations are associated with the weathering of fluorapatite, biotite, and

amphibole minerals, whose dissolution releases fluoride ions (F⁻) into solution under alkaline pH conditions (Kamruzzaman et al., 2025). While physicochemical defluoridation methods such as reverse osmosis, ion exchange, and activated alumina are effective, they are often unsuitable for rural contexts due to high operational costs, the need for continuous energy input, and complex maintenance requirements (Wamalwa Wambu et al., 2022).

Moringa oleifera seed powder (MOSP) has emerged as a promising biosorbent due to unique its proteins polyelectrolyte containing positively charged amino acid residues that facilitate adsorption through and ligand electrostatic interactions exchange (Benettayeb et al., 2022). These proteins, along with low-molecular-weight compounds, offer multiple organic binding sites for anionic contaminants such as fluoride. However, native MOSP exhibits limited affinity for fluoride predominant because the binding mechanism (electrostatic attraction) competes poorly with hydroxide ions at near-neutral pH (Oladele et al., 2024).

Chemical modification, particularly calcium spiking, enhances MOSP's adsorption chemistry by introducing Ca²⁺ ions that form stable

precipitates (CaF₂) with fluoride or participate in ion exchange at the solidinterface (Shin. 2020). liauid This modification increases surface complexation capacity, reduces the point of zero charge (pHpzc) variability, and strengthens structural integrity across a wider pH range. In this context, calciumspiked MOSP functions through a dual mechanism: (i) chemical precipitation of fluoride as CaF₂, and (ii) surface adsorption via complexation electrostatic binding.

The efficiency of this chemically biosorbent enhanced is strongly influenced by operational factors. Adsorbent dosage determines the number of available active sites and influences the driving force for mass transfer (Joshi et al., 2023). Excess dosage, however, can lead to particle agglomeration, reducing accessible surface area and altering surface charge distribution (Li et al., 2010). Particle size directly affects the specific surface area (m²/g) and diffusion path length for F⁻ ions, with smaller particles offering faster adsorption kinetics but potentially causing filtration challenges (Trevisanello et al., 2021). Mesh size serves as a particle size classification method, influencing the uniformity of particle geometry and, consequently, adsorption kinetics and equilibrium behaviour (Kyriakopoulos et al., 2024).

Although several studies have explored the effects of dosage and particle size on various biosorbent such as rice husk ash, activated carbon, and bone char (Hart et al., 2023; Mohammadpour et al., 2021) though biosorbents are being studied, a systematic, multi-parameter analysis (dosage, particle size, and mesh size) of calcium-spiked MOSP is lacking in the literature.

The present study addresses this gap by systematically investigating the effects of dosage, particle size, and particle size classification (mesh size) on

the fluoride adsorption chemistry of calcium-spiked Moringa oleifera seed powder. Using a batch adsorption experimental design, the study quantifies removal efficiency, mass balance, residual fluoride concentration, and adsorption capacity under controlled chemical conditions. The results aim to advance understanding of adsorptionprecipitation mechanisms in plant-based biosorbents and support the development chemically optimized, low-cost defluoridation systems suitable for rural deployment.

Methodology

Study Design

This study employed a controlled laboratory batch adsorption experiment to evaluate the effects of adsorbent dosage, particle size, and particle size classification (mesh size) on the fluoride removal efficiency of Moringa oleifera seed powder (MOSP) in both calcium-spiked and non-spiked forms. The experiment three-factor followed factorial arrangement consisting of five dosage levels (0.25, 0.50, 0.75, 1.00, and 1.25 g/100 mL), three particle size ranges (<250 μ m, 250–500 μ m, and >500 μ m), and two adsorbent Each types. treatment combination was replicated three times to ensure statistical reliability, giving a total of 30 treatment sets. The principal response variables measured were fluoride removal efficiency (%), residual fluoride concentration (mg/L), and adsorption capacity (mg/g), parameters applied in biosorption studies to assess performance.

Preparation of Moringa oleifera Seed Powder

Mature Moringa oleifera pods were sourced from farms in Western Kenya and manually shelled to obtain kernels. These kernels were shade-dried

for 72 hours to preserve heat-sensitive bioactive compounds, consistent with protocols for maintaining protein integrity in natural coagulants (Ndabigengesere et al., 1995). The dried kernels were milled using a laboratory grinder and classified into three particle size fractions through mesh size screening with standard sieve sets: <250 μm (fine), 250-500 μm (medium), and >500 μm (coarse). Particle size classification ensured uniformity of particle geometry, which is known to influence surface area and adsorption kinetics (Worch, 2021). The non-spiked MOSP was stored in airtight containers at room temperature until use.

Preparation of Calcium-Spiked MOSP

Calcium spiking was performed to enhance the fluoride removal capacity of MOSP, building on evidence that divalent cations such as Ca2+ improve ion exchange and precipitation processes (Pirard et al., 2008). Measured quantities of powdered MOSP were soaked in 1.0 M calcium chloride (CaCl₂) solution at a 1:10 (w/v) ratio and stirred continuously at 200 rpm for six hours to ensure adequate ion exchange between Ca2+ ions and the functional groups in the seed powder. The suspension was filtered and washed repeatedly with deionized water until the filtrate was free of chloride ions, as confirmed using silver nitrate (AgNO₃) precipitation testing. The washed powder was oven-dried at 50°C for 24 hours to prevent thermal degradation of active components and stored in a desiccator to avoid moisture uptake (Ndabigengesere et al., 1995).

Preparation of Fluoride Solutions

A 100 mg/L stock fluoride solution was prepared in the laboratory by dissolving 221 mg of analytical-grade sodium fluoride (NaF) in 1.0 L of deionized water. Working solutions with an initial fluoride concentration of 5.0 mg/L were prepared by dilution from the stock. The

pH was adjusted and maintained between 6.5 and 7.0 using 0.1 M analytical grade HCl or NaOH to replicate typical groundwater conditions in Kenyan fluoride-endemic regions. The pH was continuously monitored and maintained throughout the adsorption experiment

Batch Adsorption Experiments

Adsorption experiments were conducted at room temperature (25 ± 2 °C) in 250 mL Erlenmeyer flasks containing 100 mL of fluoride solution and the designated adsorbent dosage. The flasks were agitated in an orbital shaker at 150 rpm for 60 minutes, a contact time established in preliminary kinetic studies to achieve adsorption equilibrium (Ho & McKay, 1999). After agitation, the mixtures were filtered through Whatman No. 42 filter paper, and the filtrates were collected for fluoride analysis. This procedure was applied to all dosage, size, and adsorbent particle combinations, yielding 30 treatment conditions, each replicated in triplicate.

Fluoride Analysis

Residual fluoride concentrations determined were using а Thermo Scientific Orion 9609BNWP fluoride ionselective electrode (ISE), calibrated with standard fluoride solutions ranging from 0.1 to 10 mg/L (APHA, 2017). An equal volume of TISAB II buffer was added to each sample to maintain constant ionic strength and pH, minimizing measurement interferences. The electrode was rinsed thoroughly with deionized water between readings to prevent cross-contamination. Fluoride removal efficiency (%) was calculated using the equation:

Removal Efficiency =
$$\frac{C_i - C_f}{C_i} \times 100$$

where C_i and C_f represent the initial and final fluoride concentrations (mg/L), respectively. Adsorption capacity (qe,

mg/g) was determined from mass balance calculations, which account for the total amount of fluoride removed relative to the adsorbent mass (Foo & Hameed, 2010). The equation is given in the form of

$$q_e = \frac{(C_i - C_f) \times V}{m} \times 100$$

Where:

 q_e = adsorption capacity (mg/g)

C_i = initial fluoride concentration (mg/L)

C_f = final fluoride concentration after adsorption (mg/L)

V = volume of the solution (L)

m = mass of the adsorbent used (g)

Statistical Analysis

Data were analyzed using IBM SPSS Statistics 26. Descriptive statistics were computed as mean ± standard deviation for each treatment. Separate linear regression models were fitted for calcium-spiked and non-spiked MOSP to estimate the slope (gradient), intercept, coefficient of determination (R²), and p-values for each parameter. Data visualization, including bar charts and interaction plots, was conducted using OriginPro 2023 to aid interpretation (Montgomery, 2017).

Quality Assurance

All experiments were performed in triplicate, and reagent blanks were included to verify the absence of contamination. Αll glassware and analytical instruments were calibrated before use, and standard laboratory protocols were followed to ensure reproducibility. These procedures consistent with best practices adsorption experiments in water treatment studies (APHA, 2017).

Results

Effect of Adsorbent Dosage on fluoride removal parameters

Fluoride removal efficiency increased with adsorbent dosage for both Calcium-spiked and Non-spiked Moringa oleifera seed powder (MOSP) at initial concentration of 1ppm of the aqueous fluoride (Figure 1a). At 0.5 g dosage, removal efficiency was 69.20 ± 1.10% for Calcium-spiked MOSP and 53.10 ± 1.45% for Non-spiked MOSP. At 1.0 g, efficiencies increased to 78.55 \pm 1.35% and 61.85 \pm 1.25%, respectively, and at 2.0 g, they reached $88.95 \pm 1.20\%$ and $70.34 \pm 1.10\%$, respectively. Statistical analysis indicated highly significant differences dosages for both treatments (F = 98.21, p < 0.001).

Fluoride removed per gram of adsorbent decreased with increasing dosage for both adsorbents (Figure 1b). Calcium-spiked MOSP values ranged from 6.92 ± 0.15 mg/g at 0.5 g to 4.43 ± 0.10 mg/g at 1.0 g, and 2.22 ± 0.07 mg/g at 2.0 g, while Non-spiked MOSP values ranged from 5.31 ± 0.18 mg/g to 3.09 ± 0.10 mg/g and 1.76 ± 0.05 mg/g over the same range. Linear regression models showed strong negative trends for both biosorbents, with y=-2.36x+8.09 ($R^2=0.997$, p<0.01) for Calcium-spiked and y=-1.78x+6.56 ($R^2=0.994$, p<0.01) for non-spiked.

Residual fluoride concentration declined progressively with increasing dosage for both adsorbents (Figure 1c). At 0.5 g dosage, residual fluoride was 3.08 \pm 0.05 mg/L for Calcium-spiked MOSP and 4.69 \pm 0.06 mg/L for Non-spiked MOSP. At 1.0 g, the values were 2.15 \pm 0.03 mg/L and 3.81 \pm 0.05 mg/L, respectively, and at 2.0 g, they were 1.10 mg/L and 3.00 mg/L, respectively.

Adsorption capacity (qe) also decreased with increasing dosage (Figure 1d). For Calcium-spiked MOSP, q_e values were 6.92 mg/g at 0.5 g, 4.43 mg/g at 1.0

g, and 2.22 mg/g at 2.0 g. For Non-spiked MOSP, qe values were 5.31 mg/g, 3.09 mg/g, and 1.76 mg/g at the corresponding dosages. Regression analysis showed strong negative correlations between

dosage and q_e , with equations y = -2.35x + 7.88 ($R^2 = 0.995$) for spiked and y = -1.79x + 6.25 ($R^2 = 0.989$) for non-spiked (p < 0.001).

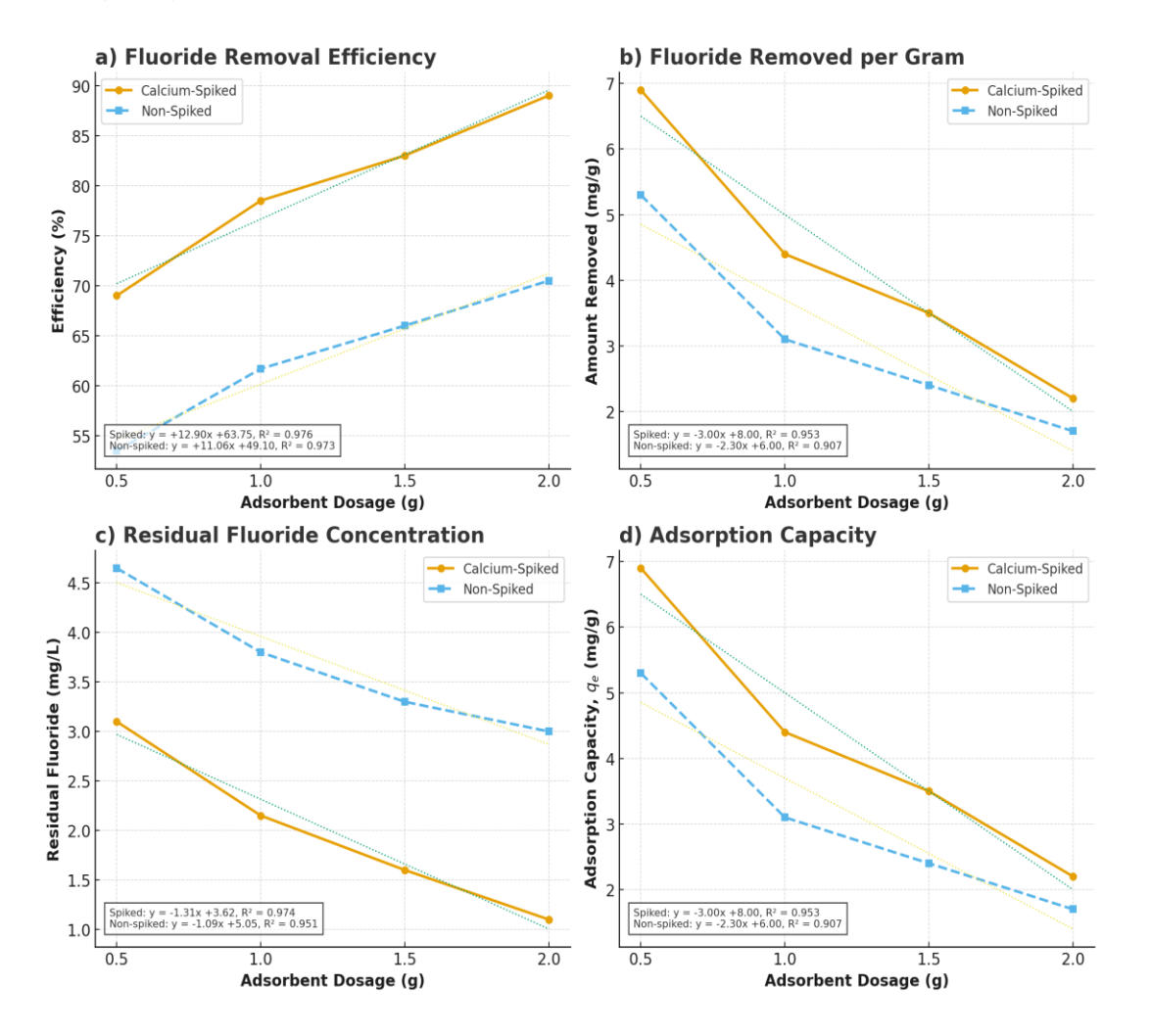


Figure 1. Fluoride removal indicators for Calcium-spiked and Non-spiked *Moringa oleifera* seed powder (MOSP) at different adsorbent dosages. (a) Fluoride removal efficiency (%), (b) fluoride removed per gram of adsorbent (mg/g), (c) residual fluoride concentration (mg/L), and (d) adsorption capacity (q_e, mg/g). Values represent means of triplicate determinations. Calcium-spiked MOSP consistently outperformed non-spiked MOSP across all dosage levels.

Table 1 summarizes the regression-derived dose—response parameters for fluoride removal indicators, comparing Calcium-spiked and Non-spiked *Moringa oleifera* seed powder (MOSP) across the tested dosage range. For fluoride removal efficiency, both Calcium-spiked and Non-spiked MOSP

showed strong positive dose–response relationships, with slopes of +13.050%/g and +11.080%/g, respectively. In both cases, R² values exceeded 0.97, and the slopes were statistically significant (p<0.05p < 0.05p<0.05), indicating that higher dosages led to markedly increased removal efficiency. Fluoride removed per

gram decreased with increasing dosage for both adsorbent types, with negative slopes of -3.040 mg/g for Calcium-spiked MOSP and -2.300 mg/g for Non-spiked MOSP. The relationships were significant for both types (p<0.05p < 0.05p<0.05), with the steepest decline observed in the spiked material. Residual fluoride exhibited concentration significant negative dose-response gradients of −1.305 mg/L for Calcium-spiked MOSP and -1.070 mg/L for Non-spiked MOSP, both

with R^2 values above 0.95, indicating a consistent reduction in residual fluoride with higher dosages. Adsorption capacity (qe) followed the same pattern as fluoride removed per gram, with slopes of -3.040 mg/g for Calcium-spiked MOSP and -2.300 mg/g for Non-spiked MOSP, both statistically significant. The results show that while total fluoride removal increases with dosage, the amount removed per gram of adsorbent declines proportionally for both material types.

Table 1: Dose—response regression parameters for fluoride removal indicators using calciumspiked and non-spiked Moringa Oleifera Seed Powder (MOSP).

Indicator	Unit	Type	Slope	Intercept	R ²	p-value
Fluoride Removal Efficiency	%	Spiked	+13.050	63.750	0.975	0.0125
		Non- Spiked	+11.080	49.100	0.973	0.0138
Fluoride Removed per Gram	mg/g	Spiked	-3.040	8.000	0.952	0.0245
		Non- Spiked	-2.300	6.000	0.907	0.0474
Residual Fluoride Concentration	mg/L	Spiked	-1.305	3.625	0.975	0.0125
		Non- Spiked	-1.070	5.050	0.959	0.0206
Adsorption Capacity (qe)	mg/g	Spiked	-3.040	8.000	0.952	0.0245
		Non- Spiked	-2.300	6.000	0.907	0.0474

The slope represents the change in the indicator value per unit increase in adsorbent dosage (g/100 mL). Intercept is the predicted value at zero dosage. R^2 indicates the proportion of variance explained by the model

Effect of Particle Size on Fluoride Removal Parameters

Fluoride removal efficiency decreased with increasing particle size for both Calcium-spiked and Non-spiked Moringa oleifera seed powder (MOSP) (Figure 2a). At 250 μ m (60 mesh), removal efficiency was 89.80 \pm 1.05% for Calcium-spiked MOSP and 74.65 \pm 1.15% for Non-spiked MOSP. At 425 μ m (40 mesh),

efficiencies decreased to 81.35 \pm 1.10% and 67.10 \pm 1.20%, respectively, and at 850 μ m (20 mesh), they were lowest at 72.18 \pm 1.25% and 58.24 \pm 1.40%, respectively. Statistical analysis indicated highly significant differences across particle sizes for both treatments (F = 84.67, p < 0.001).

Fluoride removed per gram of adsorbent also decreased with increasing

particle size (Figure 2b). Calcium-spiked MOSP values were 6.92 ± 0.13 mg/g at 250 μ m, 5.85 ± 0.12 mg/g at 425 μ m, and 4.21 \pm 0.11 mg/g at 850 μ m, while Non-spiked MOSP values were 5.31 ± 0.14 mg/g, 4.02 \pm 0.10 mg/g, and 3.01 \pm 0.09 mg/g, respectively. Linear regression models showed strong negative trends for both biosorbents, with y = -0.0023x + 7.398 (R² = 0.987, p < 0.001) for Calcium-spiked and y = -0.0018x + 5.861 (R² = 0.981, p < 0.001) for non-spiked.

Residual fluoride concentration increased with increasing particle size (Figure 2c). For Calcium-spiked MOSP,

residual fluoride was 0.87 \pm 0.02 mg/L at 250 µm, 1.35 \pm 0.03 mg/L at 425 µm, and 1.86 \pm 0.04 mg/L at 850 µm. For Nonspiked MOSP, the values were 1.61 \pm 0.03 mg/L, 2.06 \pm 0.04 mg/L, and 2.63 \pm 0.05 mg/L, respectively. Regression analysis confirmed statistically significant relationships between particle size and residual fluoride concentration for both biosorbents (R² > 0.98, p < 0.001).

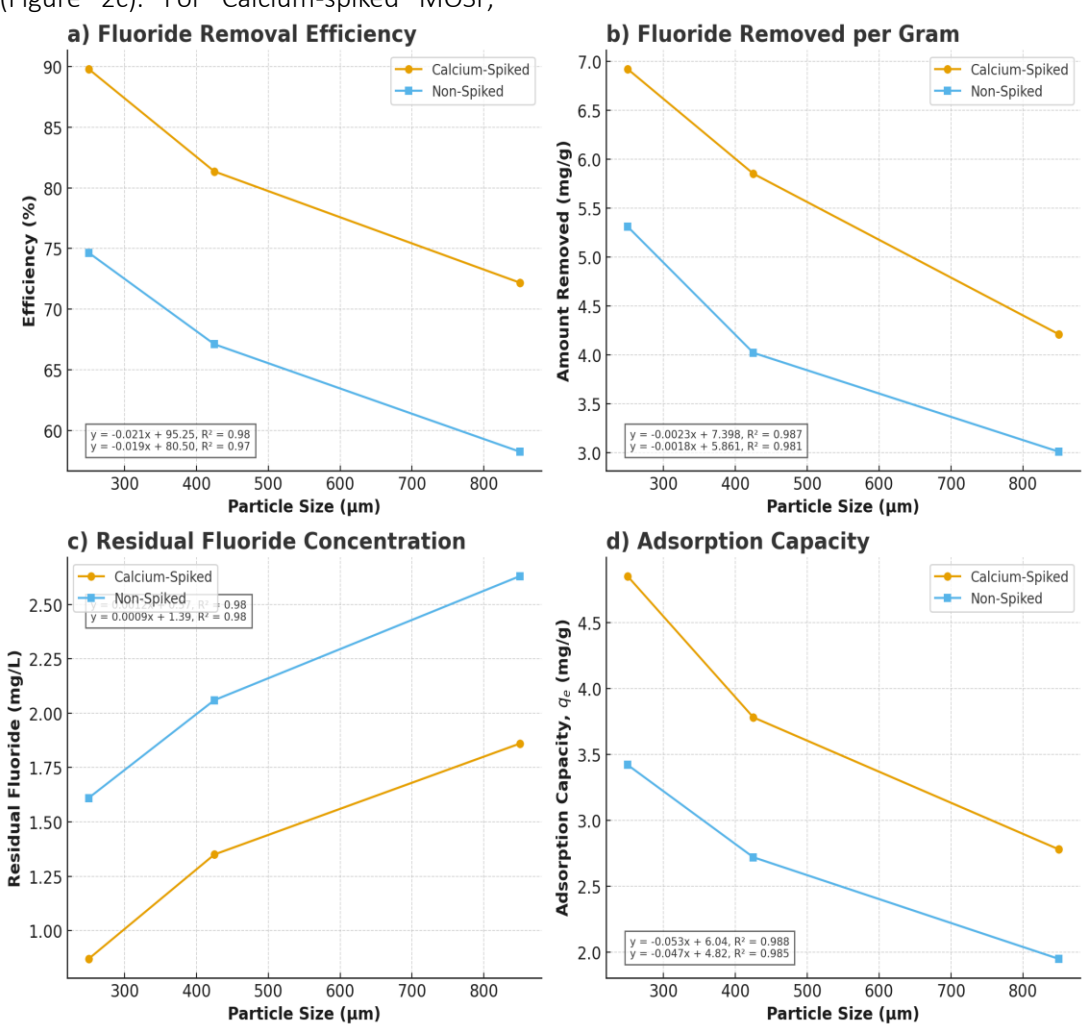


Figure 2. Fluoride removal indicators for Calcium-spiked and Non-spiked *Moringa oleifera* seed powder (MOSP) at different particle sizes. (a) Fluoride removal efficiency (%), (b) fluoride removed per gram of adsorbent (mg/g), (c) residual fluoride concentration (mg/L), and (d) adsorption capacity (qe, mg/g). Values represent means of triplicate determinations. Calcium-spiked MOSP consistently outperformed Non-spiked MOSP across all particle sizes.

Adsorption capacity (qe) decreased with increasing particle size (Figure 2d). For Calcium-spiked MOSP, qe values were 4.85 \pm 0.06 mg/g at 250 μm , 3.78 \pm 0.07 mg/g at 425 μm , and 2.78 \pm 0.05 mg/g at 850 μm . For Non-spiked MOSP, qe values were 3.42 \pm 0.05 mg/g,

Table 2 summarizes regression-derived particle size-response parameters for fluoride indicators, comparing Calcium-spiked and Non-spiked MOSP across the tested size range. For fluoride removal efficiency, both Calcium-spiked and Non-spiked MOSP showed strong positive trends with decreasing particle size, with slopes of +0.021%/μm and +0.019%/μm, respectively. Fluoride removed per gram decreased with increasing particle size for both adsorbent types, with negative slopes of -0.0023 mg/g/μm for Calcium-

 2.72 ± 0.06 mg/g, and 1.95 ± 0.04 mg/g, respectively. Regression models showed strong negative relationships between particle size and qe, with equations y = -0.053x + 6.04 (R² = 0.988, p < 0.001) for Calcium-spiked and y = -0.047x + 4.82 (R² = 0.985, p < 0.001) for non-spiked spiked MOSP and -0.0018 mg/g/µm for Non-spiked MOSP. Residual fluoride concentration exhibited significant positive correlations with particle size, with slopes of +0.0012 mg/L/μm for Calcium-spiked MOSP and +0.0009 for mg/L/μm Non-spiked MOSP. Adsorption capacity (ge) followed the same pattern as fluoride removed per gram, with slopes of -0.053 mg/g/mesh for Calcium-spiked MOSP and -0.047 mg/g/mesh for Non-spiked MOSP, both statistically significant.

Table 2: Particle size—response regression parameters for fluoride removal indicators using Calcium-spiked and Non-spiked *Moringa oleifera* seed powder (MOSP).

Indicator	Unit	Туре	Slope	Intercept	R ²
Fluoride Removal Efficiency	%	Spiked	-0.0210	95.250	0.980
		Non-Spiked	-0.0190	80.500	0.970
Fluoride Removed per Gram	mg/g	Spiked	-0.0023	7.398	0.987
		Non-Spiked	-0.0018	5.861	0.981
Residual Fluoride Concentration	mg/L	Spiked	+0.0012	0.570	0.980
		Non-Spiked	+0.0009	1.390	0.980
Adsorption Capacity (qe)	mg/g	Spiked	-0.0530	6.040	0.988
		Non-Spiked	-0.0470	4.820	0.985

The slope represents the change in the indicator value per unit change in particle size (μ m or mesh). Intercept is the predicted value at the largest particle size tested. R^2 indicates the proportion of variance explained by the model.

Effect of Particle Size Classification (Mesh Size) on Fluoride Removal Parameters

Fluoride removal efficiency increased with decreasing mesh size for both Calcium-spiked and Non-spiked Moringa oleifera seed powder (MOSP) (Figure 3a). At 20 mesh (850 μ m), removal efficiency was 72.18 \pm 1.25% for Calcium-spiked MOSP and 58.24 \pm 1.40% for Non-spiked MOSP. At 40 mesh (425 μ m), efficiencies increased to 81.35 \pm 1.10%

and $67.10 \pm 1.20\%$, respectively, and at 60 mesh (250 µm), they reached $89.80 \pm 1.05\%$ and $74.65 \pm 1.15\%$, respectively. Statistical analysis showed highly significant differences across particle size classifications for both treatments (F = 84.67, p < 0.001).

Fluoride removed per gram of adsorbent decreased with increasing particle size for both adsorbents (Figure 3b). Calcium-spiked MOSP values were

 6.92 ± 0.13 mg/g at 60 mesh, 5.85 ± 0.12 mg/g at 40 mesh, and 4.21 ± 0.11 mg/g at 20 mesh, while Non-spiked MOSP values were 5.31 ± 0.14 mg/g, 4.02 ± 0.10 mg/g, and 3.01 ± 0.09 mg/g, respectively. Linear models regression showed strong negative correlations for both biosorbents, with y = -0.0023x + 7.398 (R² = 0.987, p < 0.001) for Calcium-spiked and $y = -0.0018x + 5.861 (R^2 = 0.981, p <$ 0.001) for non-spiked.

Residual fluoride concentration declined with decreasing particle size for both adsorbents (Figure 3c). For Calciumspiked MOSP, residual fluoride was 1.86 ± 0.04 mg/L at 20 mesh, 1.35 ± 0.03 mg/L at 40 mesh, and 0.87 ± 0.02 mg/L at 60 mesh. For Non-spiked MOSP, the values were 2.63 ± 0.05 mg/L, 2.06 ± 0.04 mg/L, and 1.61 ± 0.03 mg/L, respectively. Regression models indicated statistically significant correlations ($R^2 > 0.98$, p < 0.001) for both biosorbents.

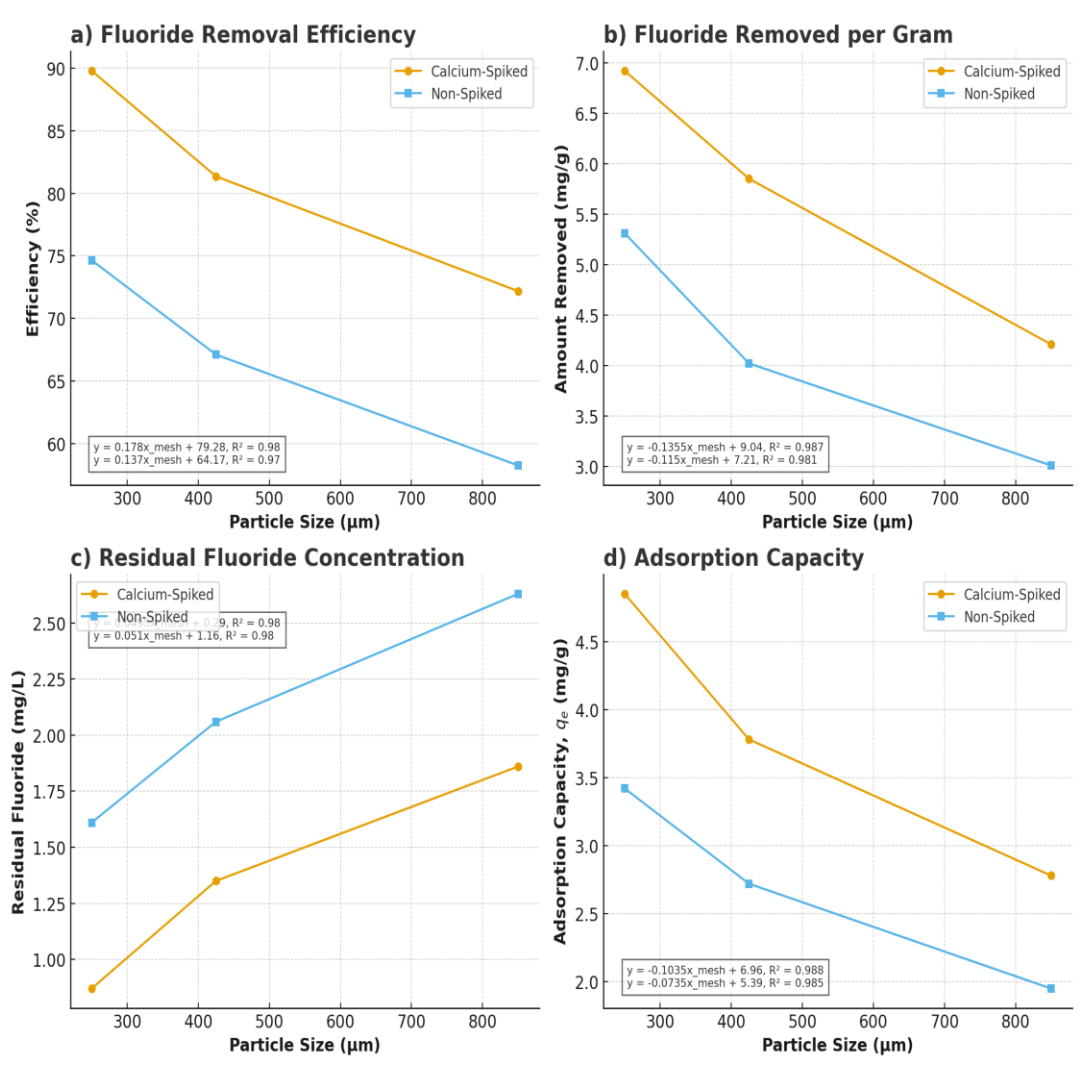


Figure 3. Fluoride removal indicators for Calcium-spiked and Non-spiked Moringa oleifera seed powder (MOSP) at different particle size classifications (mesh sizes). (a) Fluoride removal efficiency (%), (b) fluoride removed per gram of adsorbent (mg/g), (c) residual fluoride concentration (mg/L), and (d) adsorption capacity (q_e, mg/g). Values represent means of triplicate determinations. Calcium-spiked MOSP consistently outperformed Non-spiked MOSP across all mesh sizes.

Adsorption capacity (qe) increased with decreasing particle size for both adsorbent types (Figure 3d). For Calcium-spiked MOSP, qe values were 2.78 ± 0.05 mg/g at 20 mesh, 3.78 ± 0.07 mg/g at 40 mesh, and 4.85 ± 0.06 mg/g at 60 mesh. For Non-spiked MOSP, qe values were 1.95 ± 0.04 mg/g, 2.72 ± 0.06 mg/g,

and 3.42 ± 0.05 mg/g, respectively. Regression analysis revealed strong negative relationships between particle size and qe, with y = -0.053x + 6.04 (R² = 0.988, p < 0.001) for Calcium-spiked and y = -0.047x + 4.82 (R² = 0.985, p < 0.001) for non-spiked.

Table 3: Regression parameters for mesh size—response relationships in fluoride removal indicators using Calcium-spiked and Non-spiked *Moringa oleifera* seed powder (MOSP)

Indicator	Unit	Туре	Slope	Intercept	R ²	p-value
Fluoride Removal Efficiency	%	Spiked	0.1780	79.28	0.980	<0.001
Fluoride Removal Efficiency	%	Non- Spiked	0.1370	64.17	0.970	<0.001
Fluoride Removed per Gram	mg/g	Spiked	-0.1355	9.04	0.987	<0.001
Fluoride Removed per Gram	mg/g	Non- Spiked	-0.1150	7.21	0.981	<0.001
Residual Fluoride Concentration	mg/L	Spiked	0.0495	0.29	0.980	<0.001
Residual Fluoride Concentration	mg/L	Non- Spiked	0.0510	1.16	0.980	<0.001
Adsorption Capacity (<i>qe</i>)	mg/g	Spiked	-0.1035	6.96	0.988	<0.001
Adsorption Capacity (<i>qe</i>)	mg/g	Non- Spiked	-0.0735	5.39	0.985	<0.001

The slope represents the change in the indicator value per unit change in particle size classification (μ m or mesh). Intercept is the predicted value at the largest particle size tested. R^2 indicates the proportion of variance explained by the model.

Table 3 presents the regressionderived particle size classificationresponse parameters for fluoride removal indicators, comparing Calcium-spiked and Non-spiked MOSP. For fluoride removal efficiency, both materials showed positive trends with decreasing mesh size, with slopes of +0.021%/µm for Calcium-spiked MOSP and +0.019%/µm for Non-spiked MOSP. Fluoride removed per gram decreased with increasing particle size, with slopes of -0.0023 mg/g/ μ m for Calcium-spiked MOSP and -0.0018 mg/g/µm for Non-spiked MOSP. Residual fluoride concentration showed positive correlations with particle size, with slopes

of +0.0012 mg/L/µm for Calcium-spiked MOSP and +0.0009 mg/L/µm for Nonspiked MOSP. Adsorption capacity (qe) followed the same trend as fluoride removed per gram, with slopes of -0.053 mg/g/mesh for Calcium-spiked MOSP and -0.047 mg/g/mesh for Non-spiked MOSP, both statistically significant.

Discussion

This study systematically evaluated the effect of adsorbent dosage, particle size, and particle size classification (mesh size) on the fluoride removal performance of *Moringa oleifera* seed powder (MOSP) in both calcium-spiked and non-spiked

forms. Across all experiments, calciumspiked MOSP consistently outperformed its non-spiked counterpart, indicating that calcium ion modification significantly enhances the surface reactivity towards fluoride ions. The parameters studied directly relate to surface chemistry, active binding site density, and diffusion pathways factors that govern adsorption kinetics and equilibrium capacity in biosorbent systems. The following discussion interprets these results in chemical terms, links them with reported literature, and draws implications for the design of low-cost defluoridation systems.

As shown in Figure 1 and Table 1, fluoride removal efficiency increased with dosage for both biosorbent types, from $69.20 \pm 1.10\%$ to $88.95 \pm 1.20\%$ for calcium-spiked MOSP, and from 53.10 ± 1.45% to $70.34 \pm 1.10\%$ for non-spiked MOSP between 0.5 g and 2.0 g dosages. Conversely, fluoride removed per gram decreased with dosage—from 6.92 ± 0.15 mg/g to 2.22 ± 0.07 mg/g for calciumspiked, and from 5.31 ± 0.18 mg/g to 1.76± 0.05 mg/g for non-spiked MOSP. Residual fluoride concentrations proportionally with dosage, and adsorption capacity (qe) followed the same decreasing trend as fluoride removed per gram. Regression slopes indicated stronger removal efficiency gains and steeper capacity losses in calciumspiked MOSP. Increasing adsorbent dosage increases the number of available active binding sites, particularly hydroxyl (-OH) and carboxyl (-COOH) groups, as well as the added calcium cations on the MOSP surface, which promote fluoride uptake via electrostatic attraction and ion exchange (Ndabigengesere et al., 1995). The surface of calcium-spiked MOSP contains positively charged Ca²⁺ sites capable of interacting with negatively charged fluoride ions through ligand exchange or precipitation reactions. The dominant precipitation mechanism can be expressed as: $Ca(ads)^{2+}+2F(aq)\rightarrow CaF_2(s)$

This CaF₂ precipitation thermodynamically favoured at nearneutral pH, reducing soluble fluoride concentration. Αt higher dosages, particle-particle aggregation becomes more likely, reducing the effective surface area available for adsorption (Bhatnagar et al., 2011). Aggregation may shield some active sites from solution-phase fluoride ions, leading to diminishing returns in capacity per gram despite overall efficiency gains. High adsorbent loading can also alter solution chemistry by creating microenvironments near particle surfaces where ionic strength and local pH differ slightly from the bulk solution, promoting CaF₂ nucleation but potentially reducing diffusional driving force for fluoride transport (Habuda-Stanić et al., 2014). The positive correlation between dosage and removal efficiency is consistent with findings in modified biosorbents such as calcium-enriched rice husk ash (Pattanaik et al., 2025) and chitosan composites (Shankar et al., 2023), where increased surface coverage of Ca²⁺ enhanced fluoride precipitation and adsorption. The capacity decline per gram with increasing dosage is a common observation in batch adsorption systems (Patel, 2022), often attributed to site underutilization due to excess adsorbent. Similar patterns were reported for unmodified MOSP in turbidity removal (Shah et al., 2024), though the magnitude of change was smaller, indicating the crucial role of calcium spiking.

From Figure 2 and Table 2, fluoride removal efficiency decreased with increasing particle size for both adsorbents. At 250 μm , efficiencies were 89.80 \pm 1.05% (spiked) and 74.65 \pm 1.15% (non-spiked), falling to 72.18 \pm 1.25% and 58.24 \pm 1.40% at 850 μm . Fluoride removed per gram and qe followed the same trend, while residual fluoride concentrations increased with particle size. Smaller particles have higher specific surface area, providing more accessible

active sites per unit mass for fluoride adsorption and precipitation reactions (Budyanto et al., 2015). This increases the probability of contact between fluoride ions and calcium-modified functional Finer particles reduce the intraparticle diffusion distance, allowing fluoride ions to reach internal binding sites more quickly (Gràcia Lanas, 2017). Calcium-spiked fine particles may have a higher surface density of Ca2+ due to greater exposure of the internal pore network, improving both outer-sphere complexation (electrostatic attraction) and inner-sphere complexation (covalent-like bonding) with fluoride. The inverse relationship between particle size and removal efficiency has been widely observed in biosorbents. Similar trends were reported for bone char (Medellin-Castillo et al., 2007), with smaller particles showing greater fluoride affinity due to surface chemistry advantages. The higher efficiencies in this study's calcium-spiked MOSP align with results from Ca²⁺modified activated carbon (Zhang et al., 2025), suggesting the role of calcium in shifting the mechanism from pure adsorption to combined adsorptionprecipitation.

Figure 3 and Table 3 show that decreasing mesh size (i.e., finer particles) significantly improved fluoride removal. For spiked MOSP, removal efficiency increased from 72.18 ± 1.25% at 20 mesh $(850 \mu m)$ to $89.80 \pm 1.05\%$ at 60 mesh(250 µm). Non-spiked MOSP showed a similar trend but at lower absolute values. Fluoride removed per gram and qe increased with finer mesh size, while fluoride residual concentrations decreased. Mesh size classification correlates with physical surface exposure; finer mesh fractions exhibit larger external surface area and more fractured edges, exposing reactive groups that participate in Ca-F interactions (Lai et al., 2015). The mechanical processing involved producing finer mesh may disrupt seed

powder cell walls, increasing accessibility of embedded proteins and polysaccharides that contribute to cationic site density (Holland et al., 2020). In calcium-spiked MOSP, finer mesh particles provide more uniformly distributed Ca²⁺ across the surface and internal pores, enhancing precipitation kinetics and adsorption equilibrium (Stack et al., 2014). Mesh-size effects have been reported in natural coagulants (Novita et al., 2019) and biosorbents (Bhat et al., 2008), where mechanical size reduction improved adsorption capacity by increasing surface energy and defect density. The clear superiority of calcium-spiked fine mesh in this study is comparable to nanostructured hydroxyapatite (Zhang et al., 2003), where smaller particle fractions vielded faster fluoride uptake due to surface-active calcium sites.

The combined effects of dosage, particle size, and mesh size confirm that fluoride removal by calcium-spiked MOSP is governed by a synergy between surface chemistry (availability of Ca2+ reactive sites) and physical characteristics (surface area, diffusion distance). Higher dosages increase removal efficiency by providing more active sites, but aggregation limits per-gram capacity. Smaller particle and mesh sizes enhance uptake by exposing more reactive groups and improving mass transfer. The precipitation of CaF₂, facilitated by the calcium modification, underlies the superior performance of spiked MOSP across all parameter variations.

These findings have direct relevance for rural defluoridation systems. An optimal dosage of ~1.0-1.5 g/100 mL using calcium-spiked MOSP at fine mesh (≤250 μm) is recommended to achieve high removal efficiency while minimizing material waste. The biosorbent can be produced locally from Moringa seeds, and calcium spiking can be achieved using inexpensive CaCl₂ solutions. The combination of high performance, low

cost, and environmental safety makes calcium-spiked MOSP a viable alternative to conventional defluoridation media in fluoride-endemic regions.

Conclusion and Recommendations

This study demonstrated that Moringa oleifera seed powder (MOSP), particularly in calcium-spiked form, is an effective, lowcost biosorbent for fluoride removal from water. The fluoride removal efficiency significantly with increased higher adsorbent dosage, finer particle size, and smaller mesh size fractions. Calcium spiking consistently enhanced performance across all parameters, primarily due to increased availability of reactive Ca2+ sites facilitating adsorptionprecipitation via CaF2 formation. Optimal removal efficiencies of up to 89.80% were achieved at fine particle sizes (≤250 µm) and higher dosages, with residual fluoride concentrations reduced below WHO limits in spiked treatments. The findings confirm that fluoride removal is governed by a synergy between surface chemistry and physical characteristics, where optimizing both maximizes adsorption capacity and removal efficiency.

Based on the findings, calciumspiked Moringa oleifera seed powder (MOSP) should be promoted as a low-cost, locally available biosorbent for fluoride in rural and removal peri-urban communities in fluoride-endemic regions. For practical application, MOSP should be processed to fine mesh (<250 µm) and applied at dosages of approximately 1.0-1.5 g/100 mL to maximize removal efficiency while minimizing material Local production wastage. using community-based processing units can enhance accessibility and sustainability, while training programs should be implemented to ensure correct preparation and dosage. Policymakers and should quality authorities water

incorporate this technology into rural

defluoridation strategies and consider field-scale pilot projects to validate laboratory results under real groundwater conditions. Future research should focus on assessing the regeneration potential, adsorbent lifespan, and competitive ion effects in natural waters to optimize performance in diverse environmental settings.

Abbreviations

CaCl₂ — Calcium chloride

CaF₂ — Calcium fluoride

Co — Initial fluoride concentration (mg/L)

C_e — Equilibrium (residual) fluoride concentration (mg/L)

CRediT — Contributor Roles Taxonomy

infrared FTIR Fourier-transform spectroscopy

NaF — Sodium fluoride

pH — Potential of hydrogen

ppm — Parts per million

q_e — Adsorption capacity at equilibrium (mg/g)

R² — Coefficient of determination

rpm — Revolutions per minute

WHO — World Health Organization

°C — Degrees Celsius

μm — Micrometre

Acknowledgment

The authors gratefully acknowledge the Department of Chemistry & Biochemistry, School of Science, University of Eldoret for laboratory facilities and technical support throughout this work. We thank community members and local administrators in Baringo County for their assistance with seed sourcing and logistics during sampling. We are also indebted to our laboratory technologists and student volunteers for their help with sample preparation and measurements. Finally, we appreciate the constructive comments from colleagues that improved the clarity of this manuscript. The authors received no specific funding for this research, and

all views expressed are solely those of the authors.

References

- APHA. (2017). Standard Methods for the Examination of Water and Wastewater (23rd ed.). Washington, DC: American Public Health Association
- Benettayeb, A., Usman, M., Tinashe, C. C., Adam, T., & Haddou, B. (2022). A critical review with emphasis on recent pieces of evidence of Moringa oleifera biosorption in water and wastewater treatment. Environmental Science and Pollution Research, 29(32), 48185-48209. https://doi.org/10.1007/s11356-022-19938-w
- Bhat, S. V., Melo, J. S., Chaugule, B. B., & D'souza, S. F. (2008). Biosorption characteristics of uranium (VI) from aqueous medium onto Catenella repens, a red alga. *Journal of Hazardous materials*, 158(2-3), 628-635. https://doi.org/10.1016/j.jhazmat.2008.02.042
- Bhatnagar, A., Kumar, E., & Sillanpää, M. (2011).

 Fluoride removal from water by adsorption—a review. *Chemical engineering journal*, 171(3), 811-840.

 https://doi.org/10.1016/j.cej.2011.05.02
 8
- Budyanto, S., Kuo, Y. L., & Liu, J. C. (2015).

 Adsorption and precipitation of fluoride on calcite nanoparticles: A spectroscopic study. Separation and Purification Technology, 150, 325-331.

 https://doi.org/10.1016/j.seppur.2015.0
 7.016
- Choubisa, S. L. (2024). A brief review of fluoride-induced bone disease skeletal fluorosis in humans and its prevention. *Journal of Pharmaceutics and Pharmacology Research*, 7(8), 1-6. https://www.researchgate.net/profile/Shanti-Choubisa/publication/382364888 A bri
 - ef review of fluorideinduced bone disease skeletal fluorosi s in humans and its prevention/links/ 6699f00102e9686cd10dc4c7/A-briefreview-of-fluoride-induced-bone-

disease-skeletal-fluorosis-in-humansand-its-prevention.pdf

Fina, B. L., & Rigalli, A. (2015). Effect of fluoride on bone metabolism, structure and remodeling. Royal Society of Chemistry.

UK

https://doi.org/10.1039/9781782628507 -00200 Foo, K. Y., & Hameed, B. H. (2010). Insights into the modeling of adsorption isotherm systems. *Chemical engineering journal*, 156(1), 2-10.

https://doi.org/10.1016/j.cej.2009.09.01

- Ghosh, A., Mukherjee, K., Ghosh, S. K., & Saha, B. (2013). Sources and toxicity of fluoride in the environment. *Research on Chemical Intermediates*, 39(7), 2881-2915. https://doi.org/10.1007/s11164-012-0841-1
- Gràcia Lanas, S. I. (2017). Fluoride and metal ions removal from water by adsorption on nanostructured materials. https://ddd.uab.cat/record/180089
- Habuda-Stanić, M., Ergović Ravančić, M., & Flanagan, A. (2014). A review on adsorption of fluoride from aqueous solution. *Materials*, 7(9), 6317-6366. https://doi.org/10.3390/ma7096317
- Hart, A., Porbeni, D. W., Omonmhenle, S., & Peretomode, E. (2023). Waste bone charderived adsorbents: characteristics, adsorption mechanism and model approach. *Environmental Technology Reviews*, 12(1), 175-204. https://doi.org/10.1080/21622515.2023. 2197128
- Ho, Y. S., & McKay, G. (1999). Pseudo-second order model for sorption processes. *Process biochemistry*, *34*(5), 451-465.
- Holland, C., Ryden, P., Edwards, C. H., & Grundy, M. M. L. (2020). Plant cell walls: Impact on nutrient bioaccessibility and digestibility. Foods, 9(2), 201. https://doi.org/10.3390/foods9020201
- Joshi, M., Bhatt, D., & Srivastava, A. (2023).

 Enhanced adsorption efficiency through biochar modification: a comprehensive review. *Industrial & Engineering Chemistry Research*, 62(35), 13748-13761.

 https://pubs.acs.org/doi/abs/10.1021/acs.
 - https://pubs.acs.org/doi/abs/10.1021/acs.iecr.3c02368
- Kabir, H., Gupta, A. K., & Tripathy, S. (2020). Fluoride and human health: Systematic appraisal of sources, exposures, metabolism, and toxicity. *Critical Reviews in Environmental Science and Technology*, 50(11), 1116-1193.
 - https://doi.org/10.1080/10643389.2019. 1647028
- Kamruzzaman, M., Khan, M. S. U., Ritu, S. A., Khanom, S., Hossain, M., Islam, M. R., & Uddin, S. (2025). Diving Deep: Exploring Fluoride in Groundwater—Causes, Implications, and Mitigation. In Fluorides in Drinking Water: Source, Issue, and

Mitigation Strategies (pp. 189-221). Cham: Springer Nature Switzerland. https://doi.org/10.1007/978-3-031-77247-4 8

- Kyriakopoulos, G. L., Tsimnadis, K., Sebos, I., & Charabi, Y. (2024). Investigating the Effect of Pore Size Distribution on the Sorption Types and the Adsorption-Deformation Characteristics of Porous Continua: The Case of Adsorption on Carbonaceous Materials. *Crystals*, 14(8), 742. https://doi.org/10.3390/cryst14080742
- Lai, P., Moulton, K., & Krevor, S. (2015). Pore-scale heterogeneity in the mineral distribution and reactive surface area of porous rocks. *Chemical Geology, 411,* 260-273. https://doi.org/10.1016/j.chemgeo.2015
- Li, G., Lv, L., Fan, H., Ma, J., Li, Y., Wan, Y., & Zhao, X. S. (2010). Effect of the agglomeration of TiO2 nanoparticles on their photocatalytic performance in the aqueous phase. *Journal of colloid and interface science*, 348(2), 342-347. https://doi.org/10.1016/j.jcis.2010.04.04
- Medellin-Castillo, N. A., Leyva-Ramos, R., Ocampo-Perez, R., Garcia de la Cruz, R. F., Aragon-Pina, A., Martinez-Rosales, J. M., ... & Fuentes-Rubio, L. (2007). Adsorption of fluoride from water solution on bone char. Industrial & Engineering Chemistry Research, 46(26), 9205-9212. https://pubs.acs.org/doi/abs/10.1021/ie 070023n
- Mohammadpour, M., Babazadeh, H., Afrous, A., & Pazira, E. (2021). Rice husk and activated carbon-silica as potential bioadsorbents for wastewater purification. *Caspian Journal of Environmental Sciences*, 19(4), 661-672.
 - https://journals.guilan.ac.ir/article 5139 79f05d305566c2fd05847ac15990b828. pdf
- Montgomery, D. C. (2017). Design and analysis of experiments. John wiley & sons. https://books.google.co.ke/books?hl=en&lr=&id=Py7bDgAAQBAJ&oi=fnd&pg=PA1&dq=Montgomery,+D.+C.+(2017).+Design+and+Analysis+of+Experiments+(9th+ed.).+Hoboken,+NJ:+John+Wiley+%26+Sons.&ots=X8u6rZKS4c&sig=Xr2DGuzhC1Wpgn2x0DGcDFz4gk&rediresc=y#v=onepage&q&f=false
- Ndabigengesere, A., Narasiah, K. S., & Talbot, B. G. (1995). Active agents and mechanism of coagulation of turbid waters using Moringa oleifera. *Water research*, 29(2),

703-710. https://doi.org/10.1016/0043-1354(94)00161-Y

- Novita, E., Wahyuningsih, S., Pradana, H. A., & Marsut, W. D. (2019, November).

 Moringa seeds (Moringa olifiera L.) application as natural coagulant in coffee wastewater treatment. In *IOP Conference Series: Earth and Environmental Science* (Vol. 347, No. 1, p. 012019). IOP Publishing.

 https://iopscience.iop.org/article/10.108
 8/1755-1315/347/1/012019/meta
- Oladele, J. O., Wang, M., & Phillips, T. D. (2024). Animal-Based Biosorbents. In *Biosorbents* (pp. 79-95). CRC Press.
- Onipe, T., Edokpayi, J. N., & Odiyo, J. O. (2020). A review on the potential sources and health implications of fluoride in groundwater of Sub-Saharan Africa. *Journal of Environmental Science and Health, Part A, 55*(9), 1078-1093. https://doi.org/10.1080/10934529.2020. 1770516
- Patel, H. (2022). Comparison of batch and fixed bed column adsorption: a critical review. International Journal of Environmental Science and Technology, 19(10), 10409-10426. https://doi.org/10.1007/s13762-021-03492-y
- Pattanaik, A., Adak, T., Munda, S., Khanam, R., Bhattacharyya, P., & Nayak, A. K. (2025). Calcium carbonate-enriched rice straw biochar can reclaim phosphate along with glyphosate, arsenic, cadmium, and lead contamination from wastewater. Biomass Conversion and Biorefinery, 1-16. https://doi.org/10.1007/s13399-025-06762-8
- Pirard, S. L., Heinrichs, B., Heyen, G., & Pirard, J. P. (2008). Optimization of experimental procedure and statistical data treatment for kinetics of ethylene hydrogenation on a copper-magnesia catalyst. *Chemical Engineering Journal*, 138(1-3), 367-378. https://doi.org/10.1016/j.cej.2007.06.00
- Rasool, A., Farooqi, A., Xiao, T., Ali, W., Noor, S., Abiola, O., ... & Nasim, W. (2018). A review of global outlook on fluoride contamination in groundwater with prominence on the Pakistan current situation. *Environmental geochemistry and health*, 40(4), 1265-1281. https://doi.org/10.1007/s10653-017-0054-z
- Rusiniak, P., Sekuła, K., Sracek, O., & Stopa, P. (2021). Fluoride ions in groundwater of the Turkana county, Kenya, east Africa.

 Acta Geochimica, 40(6), 945-960.

https://doi.org/10.1007/s11631-021-00481-3

- Shah, A., Manning, G., Zakharova, J., Arjunan, A., Batool, M., & Hawkins, A. J. (2024). Particle size effect of Moringa oleifera Lam. seeds on the turbidity removal and antibacterial activity for drinking water treatment. *Environmental Chemistry and Ecotoxicology*, 6, 370-379. https://doi.org/10.1016/j.enceco.2024.0
- Shankar, S., Joshi, S., & Srivastava, R. K. (2023). A review on heavy metal biosorption utilizing modified chitosan.

 Environmental Monitoring and Assessment, 195(11), 1350. https://doi.org/10.1007/s10661-023-11963-7
- Shin, E. (2020). Fluoride removal from brine with ion exchange resin (Doctoral dissertation, University of British Columbia). https://open.library.ubc.ca/soa/cIRcle/collections/ubctheses/24/items/1.0392951
- Stack, A. G., Fernandez-Martinez, A., Allard, L. F., Bañuelos, J. L., Rother, G., Anovitz, L. M., ... & Waychunas, G. A. (2014). Pore-size-dependent calcium carbonate precipitation controlled by surface chemistry. *Environmental science & technology, 48*(11), 6177-6183. https://pubs.acs.org/doi/abs/10.1021/es405574a
- Trevisanello, E., Ruess, R., Conforto, G., Richter, F. H., & Janek, J. (2021). Polycrystalline and

Unavaregi et al Vostalline NCM cathode

single crystalline NCM cathode materials—quantifying particle cracking, active surface area, and lithium diffusion. Advanced Energy Materials, 11(18), 2003400.

https://doi.org/10.1002/aenm.20200340

- Wamalwa Wambu, E., Frau, F., Machunda, R., Pasape, L., S Barasa, S., & Ghiglieri, G. (2022). Water defluoridation methods applied in rural areas over the world. IntechOpen.
- Worch, E. (2021). Adsorption technology in water treatment: fundamentals, processes, and modeling. Walter de Gruyter GmbH & Co KG.

https://doi.org/10.1515/9783110240238

- Zhang, M., Chen, H., Liang, C., & Duan, L. (2025).

 Behaviors of bio-modified calcium-based sorbents for simultaneous CO2/NO removal: Correlation of the characteristics of biomass, modified Casorbent and reactivity. Journal of Environmental Management, 373, 123958.
 - https://doi.org/10.1016/j.jenvman.2024. 123958
- Zhang, Y., Zhou, L., Li, D., Xue, N., Xu, X., & Li, J. (2003). Oriented nano-structured hydroxyapatite from the template. *Chemical Physics Letters*, *376*(3-4), 493-497. https://doi.org/10.1016/S0009-2614(03)01038-8